

Artificial Vision System Design and Implementation based on BaSrTiO₃ & Nd₂O₃ Composite Memristors for Efficient Pattern Recognition

Hui He, Yifei Pei, Liu Chao Xiaobing Yan*

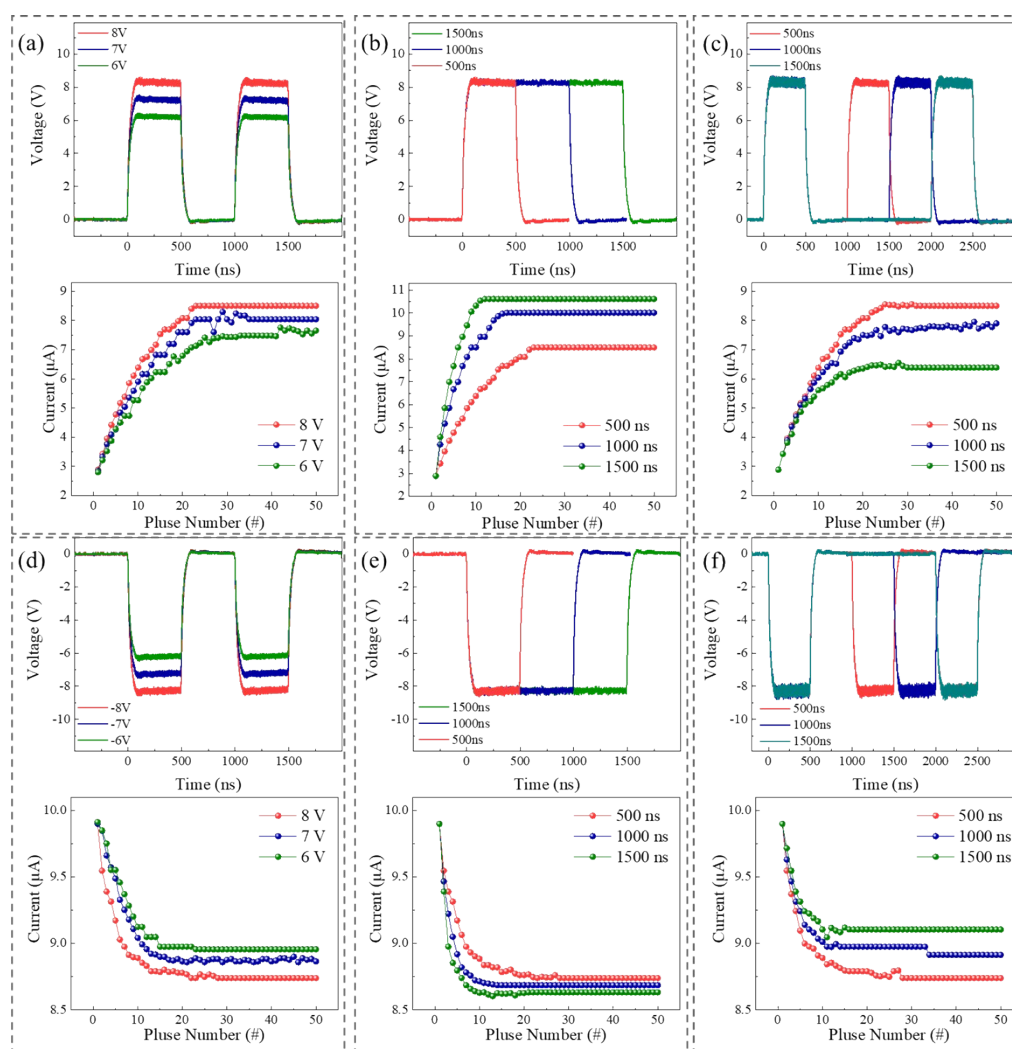


Figure S1. (a)(d) Pulse amplitude. (b)(e) Pulse width. (c)(f) Pulse interval

Figures S1a and S1d depict the resistance dependence on pulse amplitudes (ranging from 6V to 8V and -6V to -8 V). The conductance of the device exhibited more pronounced changes with increasing pulse amplitude. Subsequently, we explored the relationship between conductance variation and pulse width.^{1, 2} Figures S1b and S1e illustrate the device's conductance change after applying pulses with widths ranging from 500 ns to 1500 ns, maintaining a fixed amplitude of 8 V. The figure indicates that conductance variation becomes more prominent with increasing pulse width. Finally, figures S1c and S1f showcase the conductance change after applying pulses with intervals ranging from 500 ns to 1500 ns, again maintaining a fixed amplitude of 8 V.

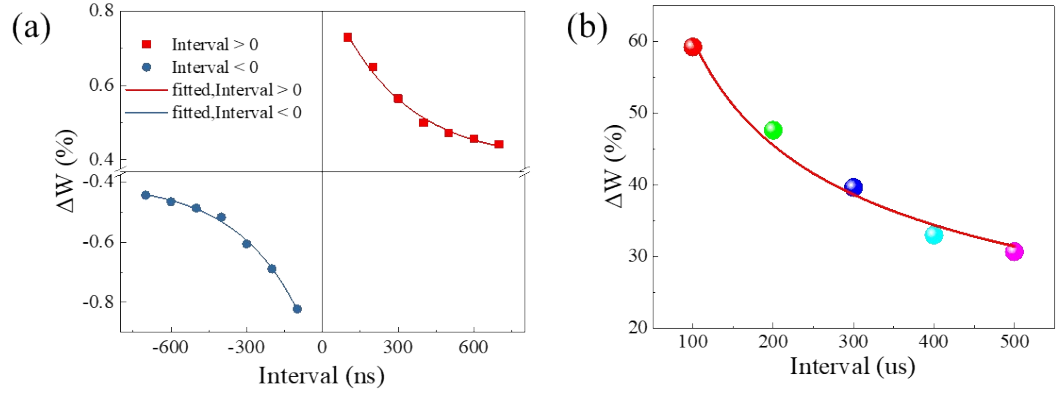


Figure S2. (a) Percentage change between synaptic weight and interval demonstrates STDP response. (b) Measured PPF index.

Figure S2a demonstrates typical STDP behavior.^{3, 4} Where synaptic weight will increase if the interval between pulses is short, known as paired-pulse facilitation (PPF),^{5, 6} as shown in Figure S2b. Our device effectively emulates both STDP and PPF learning rules. In Figure S2a, ΔW is defined as

$$\Delta W = \frac{G_2 - G_1}{G_1} \times 100\% \#$$

where G_1 and G_2 are the conductance values before and after the voltage pulse and ΔW represents the change in synaptic weight. The STDP curves were fitted using the equation

$$\Delta W = A_+ \times e^{\frac{-t}{\tau_+}}, \Delta t > 0 \#$$

$$\Delta W = A_- \times e^{\frac{-t}{\tau_-}}, \Delta t < 0 \#$$

In this work, $A_{\pm} = 0.252/-0.307$ and $\tau_{\pm} = 281.24/-253.25$.

In Figure S2b, PPF is defined as

$$PPF = \frac{G_1 - G_2}{G_1} \times 100\% = C_1 \times e^{\frac{-t}{\tau_1}} + C_2 \times e^{\frac{-t}{\tau_2}} \#$$

The fitting curve is presented in Figure S2b, where G_1 and G_2 represent the conductance after the first and second pulses, respectively. A shorter interval results in an augmentation of synaptic weight. Analyzing the fitting curves, two time constants ($\tau_1 = 62.256$ and $\tau_2 = 258.669$) were derived.

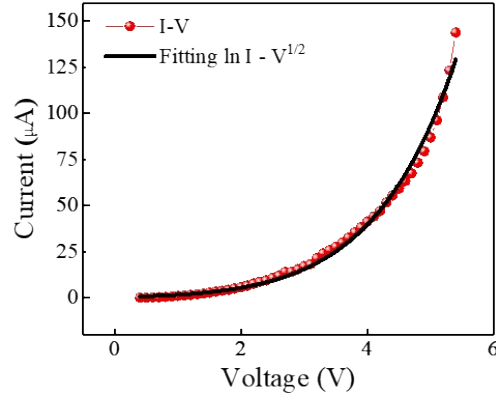


Figure S3. The IV curve is fitted using the Schottky barrier mechanism.

The Schottky barrier⁷ is a common conduction mechanism in oxide memristors, as shown in Figure S3. The device IV characteristics were fitted, and the fitting formula is as follows: $\ln I - V^{\frac{1}{2}}$.

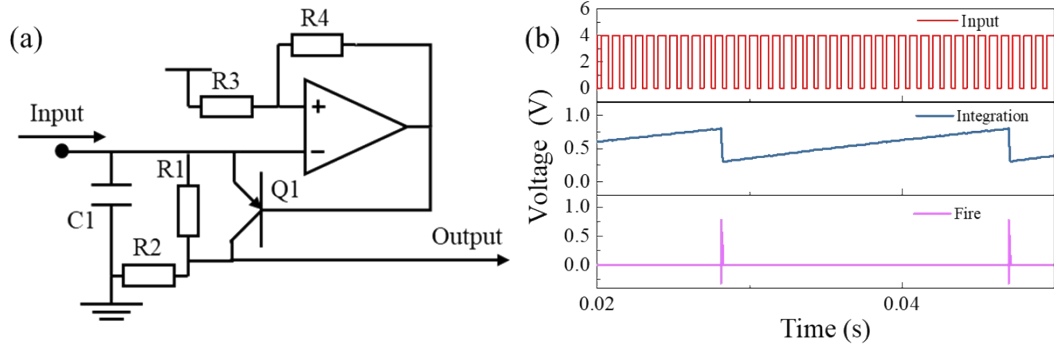


Figure S4. (a) LIF neuron circuit diagram. (b) Integrating and firing functions of neurons.

Figure S4a illustrates the LIF (leaky integrate-and-fire) neuron circuit.⁸ The integration function (I) is achieved by capacitor C1, which charges in response to the input current. The firing function (F) is implemented using a comparator to control the on/off state of the PNP transistor. When the voltage across the capacitor reaches the comparator's trigger threshold, the comparator generates a low-level output, turning on the transistor. This causes the capacitor voltage to rapidly drop through the transistor, producing a neuronal spike at the intermediate node due to the voltage division between Q1 and R2. When the input signal ceases, the voltage on C1 slowly leaks through R1 and R2 until it drops to the resting potential, simulating the leakage process (L) of biological neurons.

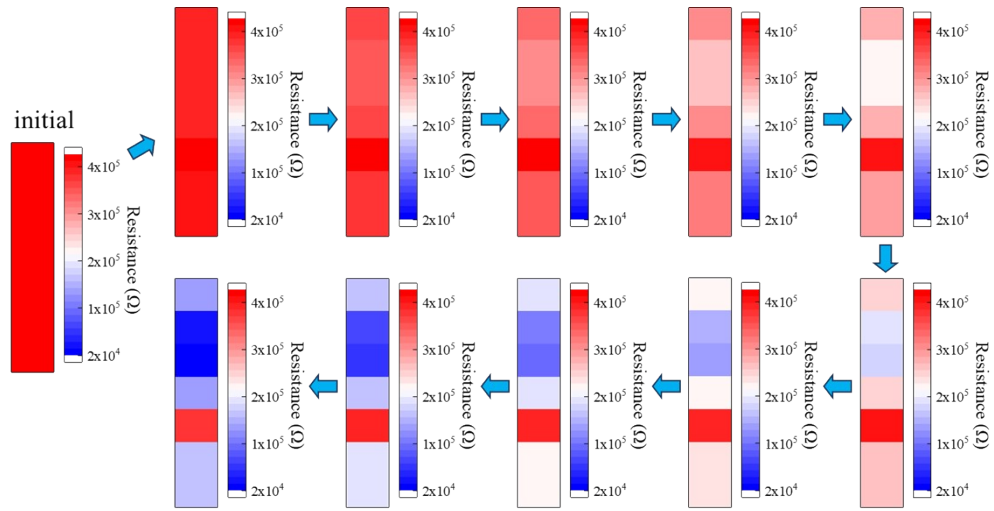


Figure S5. The process of synaptic weight changes.

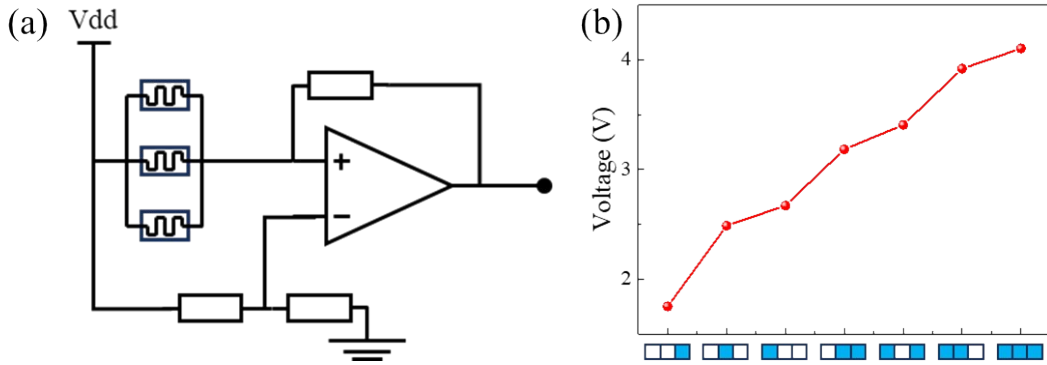


Figure S6. (a) Converter circuit diagram. Based on the principle of amplification, different voltage outputs can be produced according to the variation of the device conductance. (b) The relationship between the illumination position and the output voltage.

Operational amplifiers were used to construct a differential amplifier in the circuit. When the device's resistance decreases, the output voltage of the amplifier increases. Since the three devices are connected in parallel with different initial resistances, the change in resistance caused by light in each individual device will affect the total resistance differently, allowing the neuron to recognize these variations.

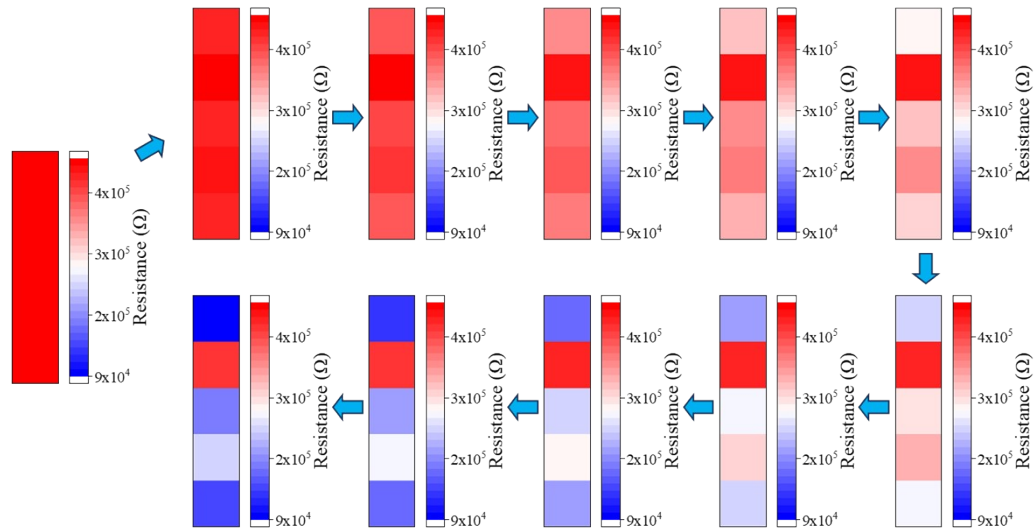


Figure S7. The process of synaptic weight changes.

1. L. Yan, Y. Pei, J. Wang, H. He, Y. Zhao, X. Li, Y. Wei and X. Yan, *Applied Physics Letters* **119** (15) (2021).
2. X. Yan, Y. Pei, H. Chen, J. Zhao, Z. Zhou, H. Wang, L. Zhang, J. Wang, X. Li and C. Qin, *Advanced materials* **31** (7), 1805284 (2019).
3. T. Serrano-Gotarredona, T. Masquelier, T. Prodromakis, G. Indiveri and B. Linares-Barranco, *Frontiers in neuroscience* **7**, 2 (2013).
4. S. R. Kheradpisheh, M. Ganjtabesh, S. J. Thorpe and T. Masquelier, *Neural Networks* **99**, 56-67 (2018).
5. C. Han, X. Han, J. Han, M. He, S. Peng, C. Zhang, X. Liu, J. Gou and J. Wang, *Advanced Functional Materials* **32** (22), 2113053 (2022).
6. S. J. Ki, J. Kim, M. Chen and X. Liang, *Applied Physics Letters* **123** (22) (2023).
7. H. Zhou, V. Sorkin, S. Chen, Z. Yu, K. W. Ang and Y. W. Zhang, *Advanced Electronic Materials* **9** (6), 2201252 (2023).
8. A. Velichko and P. Boriskov, *IEEE Transactions on Circuits and Systems II: Express Briefs* **67** (12), 3477-3481 (2020).